Thermodynamic properties of tungsten ditelluride (WTe₂)

I. The preparation and low-temperature heat capacity at temperatures from 6 K to 326 K

JANE E. CALLANAN,

Callanan Associates, 2888 Bluff, Suite 429, Boulder, CO 80301, U.S.A.

G. A. HOPE,

Griffith University, Nathan, Queensland, Australia 4111

RON D. WEIR,[a]

Department of Chemistry and Chemical Engineering, Royal Military College of Canada, Kingston, Ontario K7K 5L0, Canada

and EDGAR F. WESTRUM, JR.ᵗ

Department of Chemistry, University of Michigan, Ann Arbor, MI 48109-1055, U.S.A.

The heat capacity of the dichalcogenide: tungsten ditelluride, WTe_2, was measured over the temperature range $5.5 < T/K < 329$ using adiabatic calorimetry. Our results show that a phase transition is not present. However, an anomalous rise in the molar heat capacity $C_{p,m}$ occurs in the region $92 < T/K < 175$. The molar entropy change of this rise amounts to $\Delta S_m = (0.10 \pm 0.02) \cdot R$. The anomaly coincides with the temperature range where all the translational, librational, and internal vibrational modes become fully excited. The electronic molar heat capacity $T\gamma_m = (5.99 \pm 1.83) \, mJ \cdot K^{-1} \cdot mol^{-1}$ and, for the lattice, the Debye characteristic temperature $\Theta_D = (133.8 \pm 0.6) \, K$. Standard molar thermodynamic functions are presented at selected temperatures from 5 K to 335 K.

1. Introduction

The transition-metal dichalcogenides exhibit some remarkable properties that place them at the centre of the revolution in advanced materials suitable for engineering use, especially in hostile environments of extreme temperature and pressure. This

[a] To whom correspondence should be sent.

well-defined family of compounds has a general formula MX_2, where M is a metal element within groups 14 (IVB), 15 (VB), and 16 (VIB), and X is a chalcogen: S, Se, or Te. All members of the family crystallize into layered compounds made up of a sheet of metal atoms sandwiched between two sheets of chalcogens. Within a layer, the bonds are strong but between adjacent layers they are extremely weak. This feature gives rise to facile basic cleavage, to marked anisotropy in many of the physical properties, and to intercalation by foreign atoms. This intercalation results in the formation of new materials and in the enhancement of properties. These dichalcogenides are used, among other industrial applications, as semiconductors, components of batteries, catalysts, and high-temperature solid lubricants. It is understandable that, for the family in general, considerable work has been directed at studies of compound preparation,[1–3] crystal structure,[3–7] electronic structure,[3, 7 13] electrical and transport properties,[1, 14–22] magnetic and optical properties,[2, 23–26] and thermal stability.[27–29] However, relatively little has been published on the thermodynamic properties.[30]

Tungsten ditelluride is orthorhombic with space group Pnma, $Pnm2_1$ or No. 62 D_{2h}^{16}, lattice parameters: $a = 0.6282$ nm, $b = 0.3496$ nm, $c = 1.407$ nm. The structure shows a distorted octahedral coordination about the tungsten atom, and is isostructural with the high-temperature form of $MoTe_2$.[5] Displacement of the tungsten atoms from the centres of the octahedra to form chains extending through the crystal results in buckled layers. The displacement of the tungsten atoms increases the metallic bonding[5, 11] and facilitates conduction in WTe_2, as does the electronic band structure.[3] These effects lead to greater electrical conductivity for WTe_2 than for other group 14, 15, and 16 dichalcogenides and the classification of WTe_2 as a semi-metal.[7, 25] A thorough review of the preparation, structure, properties, and uses of WTe_2 has been published.[31] The absence of thermodynamic quantities in general, heat capacity and entropy in particular, led us to investigate these properties. In this paper, we report for the first time the results of adiabatic heat-capacity measurements on WTe_2.

2. Experimental

Crystals of WTe_2 were grown at Griffith University by vapour transport from the elements in a sealed quartz tube. The starting materials were high-purity tungsten powder (ESP1, 45 μm to 75 μm, 99.99 mass per cent) and tellurium powder (Alfa Products, 125 μm, 99.5 mass per cent). The tungsten was heated to redness in a vacuum of $<10^{-6}$ Pa to remove surface oxides. The tellurium was cleaned by washing in HCl(aq), distilled water, and ethanol, and dried in nitrogen prior to use. Stoichiometric quantities of tungsten and tellurium (25 g total) were placed into a 20 cm long quartz tube 16 mm diameter and the pressure in the tube was reduced below 1.3 mPa with a turbomolecular-pumped vacuum system. The pumping was continued for 14 h whilst the (tungsten + tellurium) powder was held at 423 K to remove water adsorbed on the surface and other volatile contaminants. Following this treatment, the tube was filled with dry $N_2(g)$ and transferred to a glovebox where the transport agent: 0.1 g of $TeCl_4$ (Aldrich, 99 mass per cent), was introduced. The

tube was then evacuated to a base pressure of $<1.3\ \mu$Pa for 24 h at ambient temperature after which it was sealed under vacuum and placed in a horizontal tube furnace.

The elements were reacted by holding the furnace temperature at 1073 K. Initially, at this temperature, the tellurium melted, and reaction with tungsten was observed over a period of several hours. No tellurium was observed in the tube after 2 d, and the reaction product was then shaken vigorously to form a powder that was distributed along the tube bottom. Crystals of WTe$_2$ were grown by maintaining the uppermost furnace temperature at 1173 K for 5 d, with crystals being evenly distributed over the tube length. The quartz tube was removed from the furnace and the product tapped to one end, and the other end of the tube held under running water to condense the transport agent and other volatile components. The WTe$_2$ crystals were recovered by breaking the ampoule, then washed with H$_2$O, and dried in vacuum. Other washing agents were not used because they intercalate readily into the telluride.[32] Surface analysis with X-ray photoelectron spectroscopy and Auger electron spectroscopy identified only tungsten and tellurium in the spectra of the crystals.

When received at the Royal Military College, the sample was placed within a quartz tube fitted with a cone and sealed socket, which contained four holes (0.5 mm) to permit evacuation. This unit was then loaded within a Pyrex tube, placed in a furnace and connected to the vacuum line, where the pressure was maintained at 1 μPa for 4 d at ambient temperature and an additional 2 d at about 575 K, which is below the range of 675 K to 875 K where decomposition is known to occur.[28,31] The tubes were opened at ambient temperature within a dry box and an 80 mg loss in the sample mass of 21 g was determined.

Crystals were removed for X-ray study and the Guinier-de Wolff diffraction pattern was in agreement with the standard pattern for WTe$_2$: No. 24-1352 as determined by the Joint Committee for Powder Diffraction Standards.[2] Its structure was found to be orthorhombic at room temperature with $a = (0.3486 \pm 0.0001)$ nm, $b = (0.6266 \pm 0.0001)$ nm, $c = (1.4045 \pm 0.0015)$ nm. The scattering pattern showed that no impurities were present.

The molar heat capacity $C_{p,\mathrm{m}}$ was measured at temperatures from 5.5 K to 329 K by adiabatic calorimetry in the Mark XIII adiabatic cryostat, which is an upgraded version of the Mark II cryostat described previously.[33] A guard shield was incorporated around the adiabatic shield. A capsule-type platinum resistance thermometer (laboratory designation A-5) was used for the temperature measurements. The thermometer was calibrated at the U.S. National Bureau of Standards (N.B.S., now NIST) against the IPTS-1948 (as revised in 1960)[34] for temperatures above 90 K, against the 1955 N.B.S. (NIST) provisional scale from 10 K to 90 K, and by the technique of McCrackin and Chang[35] below 10 K. These calibrations are judged to reproduce thermodynamic temperatures to within 0.03 K between 10 K and 90 K and within 0.04 K above 90 K.[36] The effects of changing the temperature scale to ITS-90 vary over the range $90 \leqslant T/\mathrm{K} \leqslant 350$ from $0.020 \leqslant (T_{90} - T_{48})/\mathrm{K} \leqslant -0.27$, and for the range $14 \leqslant T/\mathrm{K} \leqslant 90$ from $-0.008 \leqslant (T_{90} - T_{55})/\mathrm{K} \leqslant 0.018$.[37,38] The changes in heat capacity, enthalpy, and entropy

resulting from the conversion from IPTS-68 to ITS-90 have been shown for a number of materials to lie within the experimental error of the measurements over the range from 14 K to 2150 K.[37] Measurements of mass, current, potential difference, and time were based upon calibrations done at the N.B.S. (NIST). The heat capacities at temperatures from about 6 K to 329 K were acquired with the assistance of a computer,[39,40] which was programmed for a series of determinations. During the drift periods, both the calorimetric temperature and the first and second derivatives of temperature with respect to time were recorded to establish the equilibrium temperature of the calorimeter before and after the energy input. While the calorimeter heater was on, the heater current and potential difference as well as the duration of the heating interval were determined. Also recorded was the apparent heat capacity of the system, which included the calorimeter, heater, thermometer, and sample.

A gold-plated copper calorimeter (laboratory designation W-139) with four internal vertical vanes and a central entrant well for (heater + thermometer) was loaded with WTe_2. Following the loading, the calorimeter was evacuated and pumping was continued for several hours to ensure that moisture was no longer released from the sample. After addition of about 30 kPa (at 293 K) of helium gas so as to facilitate thermal equilibration, the vessel was then sealed by means of an annealed gold gasket tightly pressed on to the stainless-steel knife edge of the calorimeter top using a screw closure about 5 mm in diameter.

Buoyancy corrections were calculated on the basis of a crystallographic density of $9.509 \text{ g} \cdot \text{cm}^{-3}$, derived from the X-ray diffraction of our sample. The mass of WTe_2 was 20.796 70 g ($\cong 0.0473\,6749$ mol) based on its molar mass of $439.05 \text{ g} \cdot \text{mol}^{-1}$ as calculated from the 1985 IUPAC recommended atomic masses of the elements.[41]

The thermal history of the WTe_2 is represented by the following linear array. The arrows denote either cooling or heating, which correspond to the acquisition of heat-capacity results.

$$300 \text{ K} \xrightarrow{13\text{ h}} 55 \text{ K} \xrightarrow{4\text{ h}} 5 \text{ K} \underset{\text{Series I}}{\xrightarrow{8\text{ h}}} 60 \text{ K} \underset{\text{Series II}}{\xrightarrow{5\text{ h}}} 127 \text{ K}$$

$$\underset{\text{Series III}}{\xrightarrow{6\text{ h}}} 209 \text{ K} \underset{\text{Series IV}}{\xrightarrow{7\text{ h}}} 329 \text{ K}.$$

3. Results

The experimental molar heat capacities $C_{p,m}$ of our WTe_2 sample are presented in table 1, where the results are listed in order of increasing temperature. The measurements were made in four series beginning at 5.5 K and ending at 329 K. The probable errors in heat capacity decrease from about 1 per cent at 10 K to less than 0.15 per cent at temperatures above 30 K. The heat capacity of the sample varied from 0.58 at 15 K down to 0.29 at 250 K of the total heat capacity of the sample plus the calorimeter vessel.

Shown in figure 1 is the experimental $C_{p,m}/R$ (where R is the gas constant) plot for WTe_2 from 6 K to 326 K. One anomaly appears in the heat-capacity curve.

TABLE 1. Experimental molar heat capacity of WTe$_2$ ($M = 439.05$ g·mol^{-1}, $R = 8.31451$ J·K^{-1}·mol^{-1})

T/K	$C_{p,m}/R$	T/K	$C_{p,m}/R$	T/K	$C_{p,m}/R$	T/K	$C_{p,m}/R$	T/K	$C_{p,m}/R$	T/K	$C_{p,m}/R$
6.04	0.028	23.87	1.031	58.07	4.905	117.35	8.525	185.27	9.018	261.15	9.142
7.28	0.042	25.60	1.197	61.96	5.335	121.90	8.633	190.44	9.044	266.61	9.174
8.55	0.066	27.35	1.392	65.87	5.700	126.53	8.724	195.80	9.051	272.12	9.192
9.36	0.084	29.11	1.558	69.67	5.992	129.68	8.768	201.12	9.052	277.65	9.220
10.22	0.109	30.91	1.743	73.78	6.318	135.27	8.857	206.44	9.057	283.18	9.245
11.39	0.154	32.71	1.912	78.17	6.651	140.27	8.904	211.64	9.060	288.65	9.271
12.59	0.204	34.79	2.101	82.50	6.934	145.15	8.929	216.90	9.063	296.83	9.324
13.78	0.266	37.05	2.384	86.78	7.190	150.04	8.946	222.33	9.064	304.99	9.361
15.08	0.349	39.32	2.672	91.05	7.409	154.97	8.964	227.91	9.071	310.31	9.383
16.47	0.444	41.84	3.006	95.45	7.644	159.87	8.952	233.48	9.074	315.66	9.403
17.90	0.541	44.60	3.314	99.74	7.856	164.88	8.955	239.07	9.080	320.97	9.421
19.34	0.642	47.38	3.629	104.04	8.066	170.03	8.967	244.64	9.093	326.41	9.437
20.80	0.752	50.62	4.071	108.43	8.245	175.15	8.991	250.15	9.099		
22.28	0.877	54.32	4.486	112.87	8.389	180.22	9.017	255.66	9.116		

The standard molar thermodynamic functions are presented at selected temperatures in table 2. The heat capacities below 8 K were obtained by fitting our experimental values below 18 K to the limiting form of the Debye equation that included a term due to electronic conduction (see section 4). Plots of $C_{p,m}/T$ against
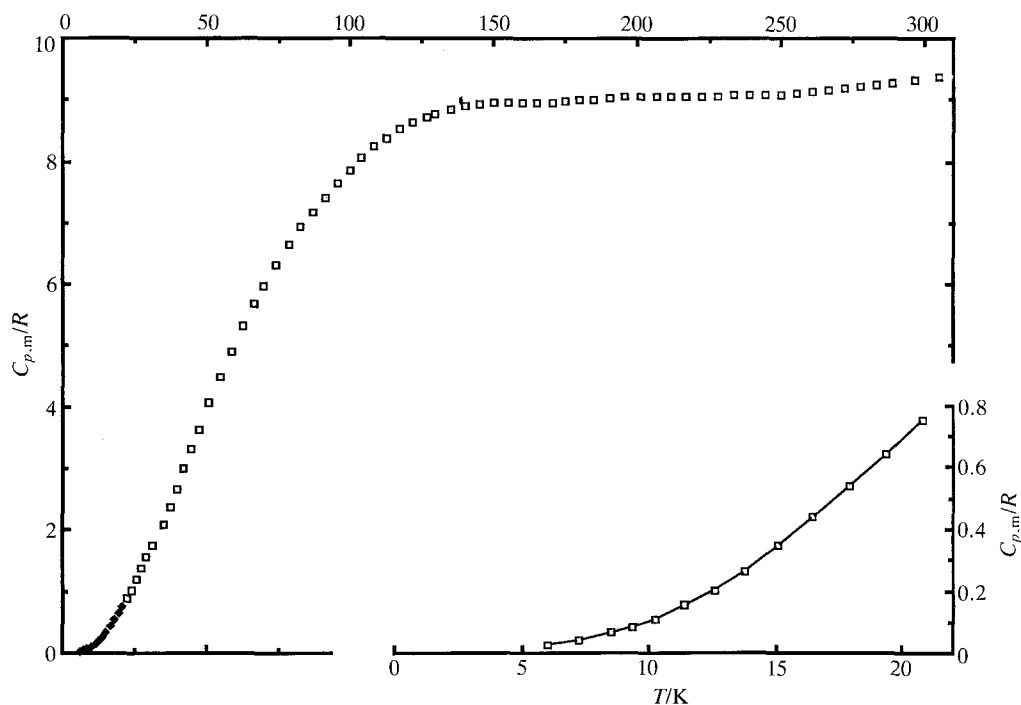
FIGURE 1. Experimental molar heat capacities $C_{p,m}$ at constant pressure plotted against temperature T for WTe$_2$. The region below $T = 22$ K is enlarged in the lower right-hand corner.

TABLE 2. Standard molar thermodynamic functions for WTe_2

$(M = 439.05 \text{ g} \cdot \text{mol}^{-1}; \ p^\circ = 101.325 \text{ kPa}; \ R = 8.31451 \text{ J} \cdot \text{K}^{-1} \cdot \text{mol}^{-1}; \ \Phi_m^\circ \overset{\text{def}}{=} -\Delta_0^T H_m^\circ / T + \Delta_0^T S_m^\circ)$

$\dfrac{T}{K}$	$\dfrac{C_{p,m}}{R}$	$\dfrac{\Delta_0^T S_m^\circ}{R}$	$\dfrac{\Delta_0^T H_m^\circ}{R \cdot K}$	$\dfrac{\Phi_m^\circ}{R}$	$\dfrac{T}{K}$	$\dfrac{C_{p,m}}{R}$	$\dfrac{\Delta_0^T S_m^\circ}{R}$	$\dfrac{\Delta_0^T H_m^\circ}{R \cdot K}$	$\dfrac{\Phi_m^\circ}{R}$
5	(0.016)	(0.0072)	(0.025)	(0.0023)	160	8.955	10.31	903.0	4.665
10	0.105	0.039	0.280	0.0111		(8.900)	(10.21)	(890.6)	(4.643)
15	0.348	0.120	1.32	0.0321	165	8.959	10.58	947.8	4.840
20	0.692	0.265	3.89	0.0709		(8.937)	(10.48)	(935.2)	(4.816)
25	1.140	0.465	8.41	0.1288	170	8.972	10.85	992.6	5.013
30	1.653	0.718	15.39	0.2053		(8.966)	(10.75)	(979.9)	(4.986)
35	2.135	1.009	24.86	0.2989	175	8.989	11.11	1037.5	5.184
40	2.760	1.334	37.05	0.4076		(8.989)	(11.01)	(1024.8)	(5.155)
45	3.360	1.694	52.37	0.5301	180	9.006	11.37	1082.5	5.352
50	3.950	2.078	70.63	0.6655		(9.006)	(11.26)	(1069.8)	(5.321)
55	4.555	2.484	91.93	0.8121	190	9.034	11.85	1172.7	5.682
60	5.146	2.905	116.1	0.9688		(9.034)	(11.75)	(1160.0)	(5.647)
65	5.608	3.335	143.0	1.134	200	9.054	12.31	1263.1	6.002
70	6.023	3.766	172.1	1.307		(9.054)	(12.22)	(1250.5)	(5.964)
75	6.421	4.195	203.2	1.485	210	9.057	12.76	1353.7	6.313
80	6.778	4.621	236.3	1.668		(9.057)	(12.66)	(1341.8)	(6.272)
85	7.080	5.041	270.9	1.854	220	9.064	13.18	1444.3	6.616
90	7.352	5.454	307.0	2.043		(9.064)	(13.08)	(1431.6)	(6.572)
92	7.460	5.617	321.9	2.118	230	9.070	13.58	1535.0	6.910
	(7.445)[a]	(5.617)	(321.8)	(2.118)		(9.070)	(13.48)	(1522.3)	(6.864)
95	7.638	5.859	344.5	2.233	240	9.082	13.97	1625.7	7.197
	(7.570)	(5.858)	(344.4)	(2.233)		(9.082)	(13.87)	(1613.0)	(7.148)
100	7.880	6.256	383.2	2.424	250	9.098	14.34	1716.6	7.475
	(7.762)	(6.251)	(382.7)	(2.424)		(9.098)	(14.24)	(1703.9)	(7.424)
105	8.116	6.647	423.2	2.616	260	9.132	14.70	1807.7	7.746
	(7.933)	(6.634)	(421.9)	(2.615)		(9.132)	(14.60)	(1795.1)	(7.693)
110	8.310	7.029	464.3	2.808	270	9.178	15.04	1899.3	8.010
	(8.084)	(7.006)	(462.0)	(2.806)		(9.178)	(14.94)	(1886.6)	(7.955)
115	8.461	7.402	506.2	2.999	280	9.228	15.38	1991.3	8.267
	(8.217)	(7.369)	(502.7)	(2.997)		(9.228)	(15.28)	(1978.7)	(8.211)
120	8.587	7.764	548.9	3.190	290	9.282	15.70	2083.9	8.518
	(8.333)	(7.721)	(544.1)	(3.187)		(9.282)	(15.60)	(2071.2)	(8.460)
125	8.693	8.117	592.1	3.381	300	9.339	16.02	2177.0	8.763
	(8.436)	(8.063)	(586.0)	(3.375)		(9.339)	(15.92)	(2164.3)	(8.704)
130	8.782	8.459	635.7	3.569	310	9.378	16.33	2270.6	9.002
	(8.526)	(8.396)	(628.5)	(3.562)		(9.378)	(16.23)	(2257.9)	(8.941)
135	8.852	8.792	679.8	3.757	320	9.415	16.62	2364.5	9.236
	(8.610)	(8.719)	(671.3)	(3.747)		(9.415)	(16.52)	(2351.9)	(9.174)
140	8.898	9.115	724.2	3.942	330	9.446	16.92	2458.9	9.464
	(8.684)	(9.034)	(714.5)	(3.930)		(9.446)	(16.81)	(2446.2)	(9.401)
145	8.929	9.428	768.8	4.126	335	9.461	17.06	2506.1	9.576
	(8.750)	(9.340)	(758.1)	(4.111)		(9.461)	(16.96)	(2493.5)	(9.512)
150	8.945	9.731	813.5	4.308	298.15	9.330	15.96	2159.7	8.718
	(8.807)	(9.637)	(802.0)	(4.290)		±0.016	±0.03	±3.3	±0.010
155	8.952	10.02	858.2	4.488					
	(8.858)	(9.927)	(846.2)	(4.468)					

[a] Quantities in parentheses represent the values taken on the smooth background curve.

T^2 and of $(C_{p,m} - \gamma T)/T^3$ against T^2, when extrapolated to $T = 0$, both yielded identical results. It should be noted that our experimental value of $S_m^\circ(298.15 \text{ K}) = (15.96 \pm 0.03) \cdot R$ compares with the $(12.58 \pm 1.51) \cdot R$ estimated by Mills,[42] who used a known $S_m^\circ(298.15 \text{ K})$ value for the related sulphide with a correction factor.

4. Analysis and discussion

THE DEBYE CHARACTERISTIC TEMPERATURE $\Theta_D(T)$

When the Debye model is obeyed, $\Theta_D(T)$ should be constant for any crystal. However, for real crystals, this model does not normally describe the experimental observations. In many diatomic lattices and metals, Θ_D asymptotically approaches constant values at high and low temperatures and shows a minimum in Θ_D at lower temperatures between the two extremes.[43]

The Debye temperature derived from the entropy $\Theta_D^S(T)$ for crystalline argon[44,45] is a simple reference with which to compare WTe₂ (see figure 2). The decrease in Θ_D^S for argon above 20 K is due mainly to the expansion of the argon lattice. For argon, there is no ambiguity in the choice of the number of vibrations used in the calculation of Θ_D^S, namely 3 vibrations (translations) per molecule. On the other hand, when the lattice of a crystal is considered, the choice of the number of vibrations depends on which vibrations are excited in a particular range of temperature. The shape of the $\Theta_D(T)$ against T curve for molecular crystals, when
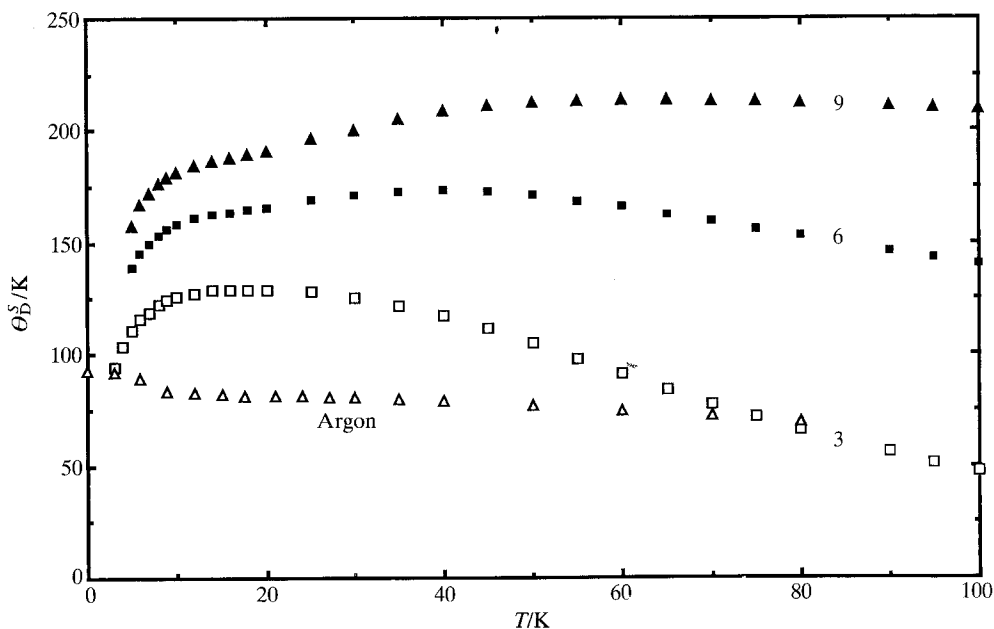
FIGURE 2. Plots of the Debye temperature $\Theta_D^S(T)$ against temperature T for different numbers of vibrational modes per molecule as shown for WTe₂. That for argon is also shown for comparison.

calculated on the basis of 3 modes per molecule, will differ from that of argon. Advantage can be taken of this to obtain qualitative information about the form of the frequency spectrum by varying the size of the vibrating unit and then examining the curves if $\Theta_D(T)$ against T in the different temperature regions.

The Θ_D^S for WTe_2, calculated using the Debye model, is plotted in figure 2 based upon three conditions of vibration, *i.e.* 3, 6, and 9 modes. Θ_D^S has been selected over Θ_D^C because Θ_D^S is less sensitive to errors in heat-capacity results, which is especially important at higher temperatures in view of our inability to make $(C_{p,m} - C_{V,m})$ corrections, as noted below. In figure 2, $\Theta_D^S(T)$ for 3 vibrations in WTe_2 rises rapidly from 3 K and gradually flattens to a constant value over the range $10 < T/K < 25$, similar to argon, implying that in this range only 3 modes contribute to the heat capacity. Above 25 K, the decline in the curve is due to the additional modes starting to contribute their energy to the heat capacity and to expansion of the WTe_2 lattice. It is this latter feature that accounts for the drop in $\Theta_D^S(T)$ for argon. The $\Theta_D^S(T)$ for the curve for 6 modes in WTe_2 begins to flatten at 25 K as the 3 librational modes become excited. Above 50 K, this $\Theta_D^S(T)$ falls off as other contributions become active and the lattice expands further. Clearly, the vibrational and librational branches of the frequency spectrum are separated in WTe_2. Above 50 K, the $\Theta_D(T)$ for 9 modes reaches a constant value as the internal vibrational modes become fully excited. As temperature rises above 100 K, the lattice continues to expand and the $(C_{p,m} - C_{V,m})$ corrections become significant.

It is evident from figure 2 that the drop in Θ_D^S at $T < 8$ K for all the WTe_2 curves makes a reliable extrapolation to obtain $\Theta_D^S(T \rightarrow 0)$ virtually impossible. Such a drop results from the failure of the Debye model to account for our heat-capacity measurements.

TEMPERATURE DEPENDENCE OF $C_{p,m}$ AT TEMPERATURES BELOW 20 K

The failure of the Debye model at $T < 10$ K noted above implies a possible contribution to the $C_{p,m}$ from a source other than the lattice vibrations. The fact that WTe_2 is known to be a conductor with interesting electrical properties[7,16,22] leads to the inclusion of an electronic term γT along with those representing the phonons.

The quantity measured calorimetrically is C_{sat}, the heat capacity of the solid in equilibrium with its saturated vapour. The background heat capacity of the vessel and helium exchange gas have been deducted from this quantity. A complete analysis of heat-capacity results over a wide temperature range requires $C_{V,m}$, which is related to $C_{sat,m}$ by

$$C_{sat,m} - C_{p,m} = (\partial p/\partial T)_{sat}\{(\partial H_m/\partial p)_T - V\}, \tag{1}$$

$$C_{p,m} - C_{V,m} = \alpha^2 V_m T/\kappa_T, \tag{2}$$

where $\alpha = V_m^{-1}(\partial V_m/\partial T)_p$ is the isobaric expansivity, V_m is the molar volume, and $\kappa_T = -V_m^{-1}(\partial V_m/\partial p)_T$ is the isothermal compressibility. The vapour pressure of solid WTe_2 is negligible so that $C_{sat,m} = C_{p,m}$ from equation (1). It should be noted that the pressure effect of the helium exchange gas on the heat capacity of solid WTe_2, *i.e.*
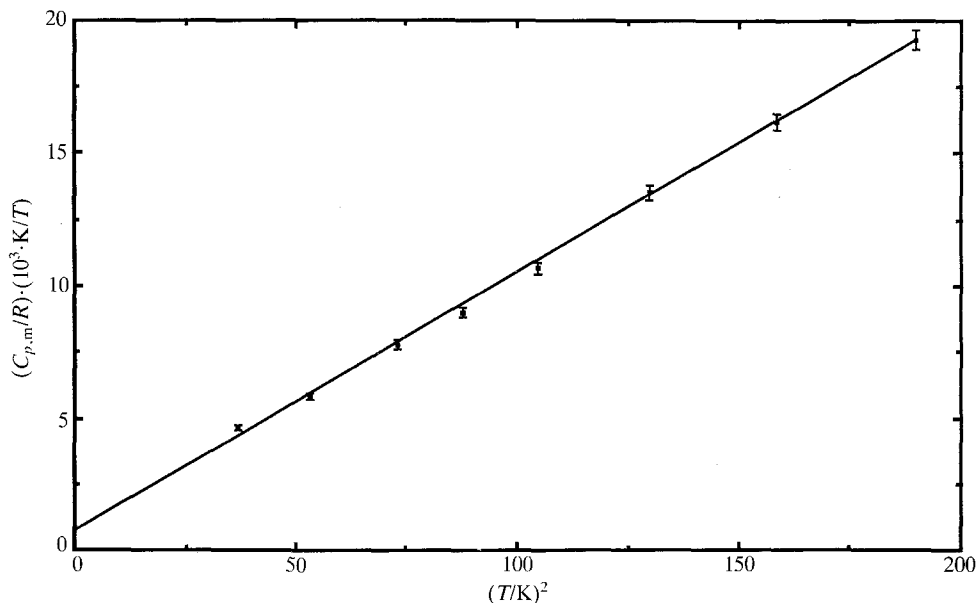
FIGURE 3. Plot for $C_{p,m}/RT$ against temperature T^2 for WTe$_2$. ⟂, $0.02(C_{p,m}/R)(10^3 \cdot \mathrm{K}/T)$.

$(\partial C_p/\partial p)_T$, is also negligible (2.0 kPa of helium at 20 K). Returning to equation (2), low-temperature values of α, V_m, and κ_T are unavailable for WTe$_2$ but fortunately at the lowest temperatures in most solids ($C_{p,m} - C_{V,m}$ becomes negligibly small.[46-48] Therefore, we have assumed that $C_{p,m} = C_{V,m}$ in the low-temperature region where our analysis is focused.

The heat capacity at very low temperature can be described by a power series of the form:

$$C_{V,m} = \gamma T + aT^3 + bT^5 + cT^7 + \cdots, \qquad (3)$$

in which the coefficient γ arises from conduction of the electrons through the lattice[49] and the coefficients a, b, and c are related directly to the coefficients in the corresponding power series for the frequency spectrum at low frequencies.[50] As $T \to 0$ is approached, the lattice heat-capacity of the solid should equal that of an elastic continuum and is described by the Debye T^3 law: $C_{V,m} = aT^3$ and $\Theta_D = (12\pi^4 Lk/5a)^{1/3}$. The Θ_D is the Debye characteristic temperature derived from heat-capacity results rather than from the entropy.

A plot of $C_{p,m}/T$ against T^2 yields as $T \to 0$ the electronic γ as the intercept and the coefficient a of the first lattice term as the slope. From figure 3, the resulting $\gamma = (0.00072 \pm 0.00022) \cdot R \cdot \mathrm{K}^{-1}$ or $(5.99 \pm 1.83)\,\mathrm{mJ} \cdot \mathrm{K}^{-2} \cdot \mathrm{mol}^{-1}$ and an $a = (8.11 \pm 0.10) \cdot 10^{-4}\,\mathrm{J} \cdot \mathrm{K}^{-4} \cdot \mathrm{mol}^{-1}$. As a check on the determination of the coefficient a, the more sensitive plot of $(C_{p,m} - \gamma T)/T^3$ against T^2 yielded an identical $a = 8.11 \cdot 10^{-4}\,\mathrm{J} \cdot \mathrm{K}^{-4} \cdot \mathrm{mol}^{-1}$ when $T^2 \to 0$. Using this value of a in equation (5), $\Theta_D^C(T \to 0) = (133.8 \pm 0.6)\,\mathrm{K}$ which compares with 93.5 K for argon.

TABLE 3. The molar electronic heat-capacity divided by temperature, γ, and electrical resistivity ρ, at the temperature 295 K to 298 K of selected solids

	$\gamma/(\text{mJ} \cdot \text{K}^{-2} \cdot \text{mol}^{-1})$	$\rho/(\mu\Omega \cdot \text{cm})$	References
Cu	0.744	1.68	49, 53, 54
Al	1.21	2.76	49, 53, 54
W	1.36	5.32	49, 53, 54
Mo	2.11	5.33	49, 53, 54
WTe_2	5.99	$2.87 \cdot 10^3$	this work, 1
WSe_2	?	$500 \cdot 10^3$	1
$MoSe_2$	0	$3440 \cdot 10^3$	1, 51
Te	0	$4360 \cdot 10^3$	49, 54, 55
$MoTe_2$	0	$8500 \cdot 10^3$	1, 51
Se	0	$10000 \cdot 10^3$	49, 54

Published values of the electronic specific heat for other chalcogenides are scarce. Those for $MoSe_2$ and $MoTe_2$ are known to be zero,[51] but that for WSe_2 cannot be derived from the published heat-capacity measurements because the latter extend down only to 71 K.[52] Compared in table 3 are values of the electronic molar heat capacity divided by temperature for selected solids together with their electrical resistivity ρ showing a correlation between very high values of ρ and $\gamma = 0$.

ANOMALOUS $C_{p,m}$ AT TEMPERATURES BETWEEN 92 K AND 175 K

Examination of the curve of heat-capacity against temperature in figure 1 shows the presence of an anomalous rise in $C_{p,m}$ above 100 K. This region of $C_{p,m}$ has been expanded in figure 4 where the smoothed background curve is also indicated. The anomalous $C_{p,m}$ begins at 92 K and ends at 175 K. The greatest difference between the experimental $C_{p,m}$ and the lower background curve occurs at 125 K and amounts to $0.03 \cdot C_{p,m}$. The molar entropy difference between the two curves from 92 K to 175 K amounts to $\Delta S_m = (0.10 \pm 0.02) \cdot R$. An absence of thermal expansivities and crystal-structure information through this temperature region hampers an explanation of the phenomenon. It is noted, however, that the onset of the anomaly occurs at a temperature where the 3 internal vibrations become fully excited.

Compared on figure 4 are the experimental $C_{p,m}$ values for the related tungsten diselenide, WSe_2.[52] An anomaly similar in shape to that found in WTe_2 is present, an anomaly not discerned by the authors of reference 52. Its range extends from about 110 K to 153 K. We have plotted the original $C_{p,m}$ results, drawn smoothed curves through the experimental points, the background curve below the anomaly, and evaluated the thermodynamic functions between 72 K and 300 K. The associated molar entropy between the experimental and background curves is $\Delta S_m = (0.020 \pm 0.090) \cdot R$. It is not unreasonable to suggest that the source of the anomaly is probably the same in both WTe_2 and WSe_2.

Similarly shaped but broader anomalies in the heat capacity have been noted for NH_4ReO_4, ND_4ReO_4, NH_4IO_4, ND_4IO_4, which crystallize in the tetragonal scheelite structure, and NH_4ClO_4 and ND_4ClO_4 which are orthorhombic.[56-60] The
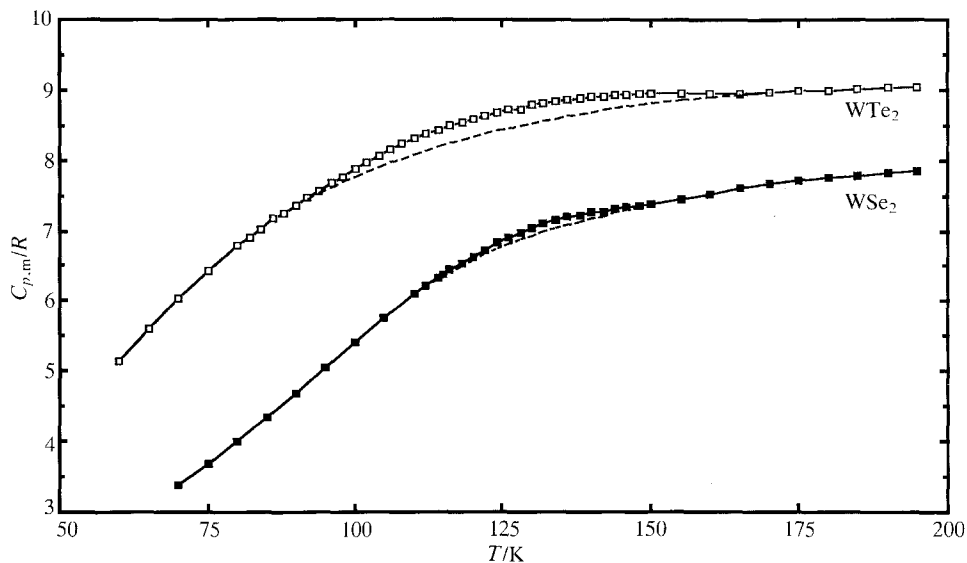
FIGURE 4. Experimental molar heat capacities $C_{p,m}$ at constant pressure plotted against temperature T for WTe$_2$ and WSe$_2$.

origins of these anomalies are thought to lie in the anisotropic thermal expansivities, which are known for these six crystals, but a final test of the hypothesis awaits measurement of the elastic constants needed to calculate the contribution to the $C_{p,m}$.[47,48,60] The fact that WTe$_2$ and WSe$_2$ are also highly anisotropic in many of their physical properties suggests this as a possible origin of the anomaly in their $C_{p,m}$. Their electrical conductivity and thermal conductivity down to at least 100 K are much greater in the plane of the layers than at right angles to the plane of the layers.[22] Unfortunately, their thermal expansivities are apparently not known.

REFERENCES

1. Brixner, L. H. *J. Inorg. Nucl. Chem.* **1962,** 24, 257.
2. Opalovskii, A. A.; Fedorov, V. E.; Lobkov, E. U.; Erenburg, B. G.; Senchenko, L. N. *Izv. Akad. Nauk SSSR, Neorg. Mater.* **1970,** 6, 561; *Inorg. Mater.* **1970,** 6, 495.
3. Mentzen, B. F.; Sienko, M. J. *Inorg. Chem.* **1976,** 15, 2198.
4. Knop, D.; Haraldsen, H. *Can. J. Chem.* **1956,** 34, 1142.
5. Brown, B. E. *Acta Cryst.* **1966,** 20, 268.
6. Clarke, R.; Marseglia, E.; Hughes, H. P. *Phil. Mag.* **1978,** 38B, 121.
7. Dawson, W. G.; Bullett, D. W. *J. Phys. C: Solid State Phys.* **1987,** 20, 6159.
8. Huisman, R.; Jonge, R. de; Haas, C.; Jellinek, F. *J. Solid State Chem.* **1971,** 3, 56.
9. Mattheiss, L. F. *Phys. Rev. Letters* **1973,** 30, 784.
10. Kasowski, R. V. *Phys. Rev. Letters* **1973,** 30, 1175.
11. Gamble, F. R. *J. Solid State Chem.* **1974,** 9, 358.

12. Madhukar, A. *Solid State Comm.* **1975**, 16, 383.
13. Manolikas, C.; Landuyt, J. van; Amelinckx, S. *Phys. Status Solidi* **1979**, 53, 327.
14. Hicks, W. T. *J. Electrochem. Soc.* **1964**, 111, 1058.
15. Champion, J. A. *Brit. J. Appl. Phys.* **1965**, 16, 1035.
16. Kabashima, S. *J. Phys. Soc. Jpn.* **1966**, 21, 945.
17. Kershaw, R.; Vlasse, M.; Wold, A. *Inorg. Chem.* **1967**, 6, 1599.
18. Upadhyayula, L. C.; Loferski, J. J.; Wold, A.; Giriat, W.; Kershaw, R. *J. Appl. Phys.* **1968**, 39, 4736.
19. Vellinga, M. B.; Jonge, R. de; Haas, C. *J. Solid State Chem.* **1970**, 2, 299.
20. El-Mahalawy, S. H.; Evans, B. L. *Phys. Status Solidi* **1977**, 79, 713; **1978**, 86, 151.
21. Hughes, H. P.; Friend, R. H. *J. Phys. C.: Solid State Phys.* **1978**, 11, L103.
22. Troadec, J. P.; Bideau, D.; Guyon, E. *J. Phys. C: Solid State Phys.* **1981**, 14, 4807.
23. Fivoz, R.; Mooser, E. *Phys. Rev.* **1967**, 163, 743.
24. Funville, R. M. M.; Geertsma, W.; Hass, C. *Phys. Status Solidi* **1978**, 85, 621.
25. Wilson, J. A.; Yoffe, A. D. *Adv. Phys.* **1969**, 169, 18.
26. Anedda, A.; Forten, E.; Roga, E. *Can. J. Phys.* **1979**, 57, 368.
27. Opalovskii, A. A.; Fedorov, V. E.; Lobkov, E. U.; Tsikanovskii, B. I. *Russ. J. Phys. Chem.* **1971**, 45, 1064.
28. Yanaki, A. A.; Obolonchik, V. A. *Zhur. Prikl. Khim.* **1974**, 47, 1454.
29. Krabbes, G. *Z. anorg. allg. Chem.* **1986**, 543, 97.
30. (a) O'Hare, P. A. G. *J. Chem. Thermodynamics* **1987**, 19, 675; (b) O'Hare, P. A. G.; Hope, G. A. *J. Chem. Thermodynamics* **1992**, 24, 639.
31. Srivastava, S. K.; Avasthi, B. N. *J. Mat. Sci.* **1985**, 20, 3801.
32. O'Hare, P. A. G.; Hope, G. A. *J. Chem. Thermodynamics* **1989**, 21, 701.
33. Westrum, E. F., Jr.; Furukawa, G. T.; McCullough, J. P. *Experimental Thermodynamics,* Vol. 1. McCullough, J. P.; Scott, D. W.: editors. Butterworths: London. **1968**, p. 133.
34. Stimson, H. F. *J. Res. Natl. Bur. Stand.* **1961**, 65A, 139.
35. McCrackin, F. L.; Chang, S. S. *Rev. Sci. Instrum.* **1975**, 46, 550.
36. Chirico, R. D.; Westrum, E. F., Jr. *J. Chem. Thermodynamics* **1980**, 12, 311.
37. Goldberg, R. N.; Weir, R. D. *Pure Appl. Chem.* in the press.
38. Bedford, R. E.; Durieux, M.; Muijlwijk, R.; Barber, C. R. *Metrologia* **1969**, 5, 47.
39 Westrum, E. F., Jr. *Proceedings NATO Advanced Study Institute on Thermochemistry at Viana do Castello, Portugal.* M. A. V. Ribiero da Silva: editor. Reidel: New York. **1984**, p. 745.
40. Andrews, J. T. S.; Norton, P. A.; Westrum, E. F., Jr. *J. Chem. Thermodynamics* **1978**, 10, 949.
41. *Pure Appl. Chem.* **1986**, 58, 1678.
42. Mills, K. C. *Thermodynamic Data for Inorganic Sulphides, Selenides, and Tellurides.* Butterworths: London. **1974**, pp. 13, 676.
43. Blackman, M. *Handb. Physik* **1955**, 7, 325.
44. Flubacher, P.; Leadbetter, A. J.; Morrison, J. A. *Proc. Phys. Soc. London* **1961**, 78, 1449.
45. Beaumont, R. H.; Chihara, H.; Morrison, J. A. *Proc. Phys. Soc. London* **1961**, 78, 1462.
46. Mountfield, K. R.; Weir, R. D. *J. Chem. Phys.* **1976**, 64, 1768.
47. Brown, R. J. C.; Callanan, J. E.; Weir, R. D.; Westrum, E. F., Jr. *J. Chem. Physics* **1986**, 85, 5963.
48. Brown, R. J. C.; Callanan, J. E.; Weir, R. D.; Westrum, E. F., Jr. *J. Chem. Thermodynamics* **1987**, 19, 1173.
49. Rosenburg, H. M. *Low Temperature Solid State Physics.* Oxford University Press: Oxford. **1963**.
50. Barron, T. H. K.; Berg, W. T.; Morrison, J. A. *Proc. Roy. Soc. London* **1957**, A242, 478.
51. Kiwia, H. L.; Westrum, E. F., Jr. *J. Chem. Thermodynamics* **1975**, 7, 683.
52. Bolgar, A. S.; Trofimova, Zh. A.; Yanaki, A. A. *Poroshk. Metal.* **1990**, 5(329), 53.
53. Cezairliyan, A.; Miller, A. P. *Specific Heat of Solids; Data Series on Material Properties,* Vol. I-2, C. Y. Ho: editor. Hemisphere: London. **1988**, p. 39.
54. White, G. K. *Experimental Techniques in Low-Temperature Physics,* 2nd edition. Oxford University Press: Oxford. **1968**, pp. 374–376.
55. Weast, R. C. *Handbook of Chemistry and Physics,* 65th edition. Chemical Rubber Publishing: Baton Raton. **1984**, p. F120.
56. Weir, R. D.; Staveley, L. A. K. *J. Chem. Phys.* **1980**, 73, 1386.
57. Brown, R. J. C.; Callanan, J. E.; Weir, R. D.; Westrum, E. F., Jr. *J. Chem. Thermodynamics* **1986**, 18, 787.
58. Brown, R. J. C.; Callanan, J. E.; Haslett, T. L.; Weir, R. D.; Westrum, E. F., Jr. *J. Chem. Thermodynamics* **1987**, 19, 711.
59. Brown, R. J. C.; Callanan, J. E.; Haslett, T. L.; Weir, R. D.; Westrum, E. F., Jr. *J. Chem. Thermodynamics* **1987**, 19, 1111.
60. Brown, R. J. C.; Weir, R. D.; Westrum, E. F., Jr. *J. Chem. Phys.* **1989**, 91, 399.